Hidden Mobile Terminal Device Discovery in a UWB Environment

Sanghoon Park, Lawrence E. Larson, and Laurence B. Milstein

Center for Wireless Communication, Dept. of Electrical and Computer Engineering,
University of California - San Diego, La Jolla, CA 92037

***Abstract* — A mobile terminal (MT) device detection technique is proposed to enhance UWB / WiMAX interoperability by measuring the low level leakage signal from a WiMAX MT local oscillator (LO). The probabilities of false alarm and missed detection are derived in order to determine the limits of detector sensitivity.**

***Index Terms* — UWB, WiMAX, interference, cognitive radio, LO leakage, discrete fourier transform, signal detection.**

I. Introduction

An ultra wide-band (UWB) signal is defined as either possessing a 20% fractional bandwidth or as a signal whose bandwidth is greater than 500 MHz, regardless of the fractional bandwidth [1]. Since a UWB signal occupies such a large bandwidth, the likelihood of its spectrum overlaying those of other wireless devices is a major concern, and so an active detection method is necessary to minimize the potential interference problems.

Worldwide interoperability for microwave access (WiMAX) is one of the systems that are expected to share the frequency spectrum with UWB devices. WiMAX technology, based on the IEEE 802.16 standard, has been developed to cover the range of up to 50 km, with a data rate of up to 70 Mbps, using orthogonal frequency division multiplexing (OFDM). Several frequency bands, ranging from 2 to 10 GHz, are currently being pursued, such as the unlicensed 5 GHz band, the licensed 3.5 GHz band, and the licensed 2.5 GHz band for wireless metropolitan area networks (W-MANs) [2]. Since nearby UWB transmitters could interfere with a WiMAX MT receiver, an MT detection scheme is desired. In this paper, such a detection technique is investigated.

II. Detection Technique

Once a WiMAX channel is set up, there are two wireless connections - downlink and uplink - between a WiMAX access point (AP) and a WiMAX mobile terminal (MT). Both of them are potentially useful for a UWB device to detect the WiMAX MT that happens to be inside its communication range, as shown in Fig. 1. The uplink connection is present when the WiMAX MT transmits a signal, and so the detection timing can be critical because the WiMAX MT device usually spends most of the time listening to the WiMAX AP. The downlink connection, on the other hand, is present more often than the uplink connection, so there are more chances for a UWB device to detect a nearby WiMAX MT when it is receiving, especially in the "idle" mode, than when it is transmitting [3].

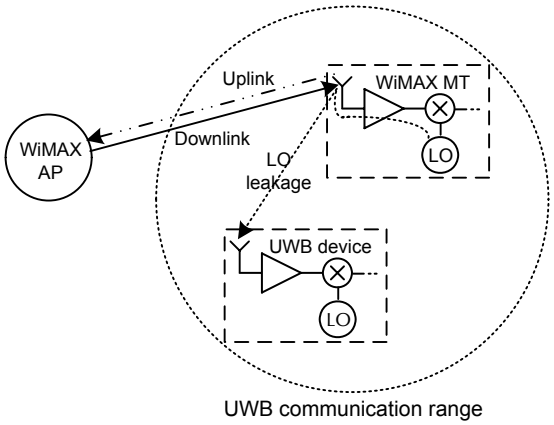

Fig. 1. Typical coexistence situation where a WiMAX MT is inside the UWB communication range.

When a WiMAX MT is receiving a signal, a small portion of the receiver local oscillator signal power in the front-end RF section leaks to the antenna and radiates. A sufficiently sensitive receiver can use this signal to determine the presence of a nearby MT receiver. The leakage signal is very weak, so the detector should have very high sensitivity. Typically, a leakage signal power level of –70 to –90 dBm is expected at the MT device antenna port [4], and a maximum path loss of 65 to 75 dB is expected in an indoor environment [5]. An existing application of LO leakage signal detection is found in television detection in the United Kingdom [6].

The proposed technique for using the leakage signal as a detection source will be useful when the WiMAX receiver employs a direct conversion type receiver, and so the unmodulated leakage signal is centered at the

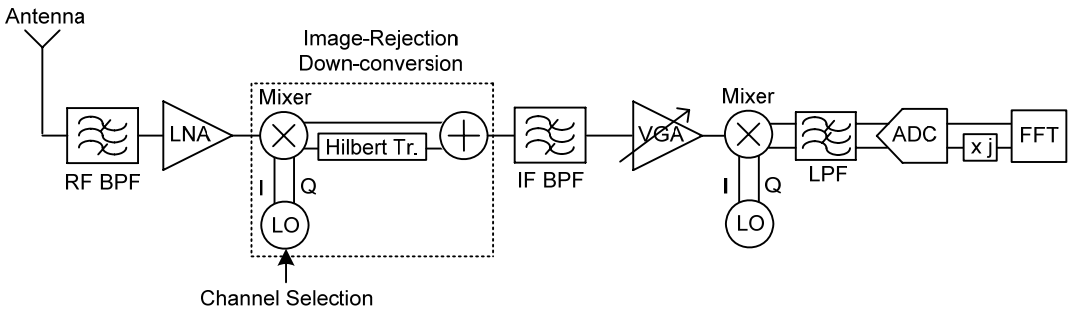

Fig. 2. Proposed detector prototype.

corresponding WiMAX channel. Therefore, a detector can directly map the spectrum information of the captured leakage signals with the occupied frequency bands of the WiMAX system. However, in case the WiMAX MT device utilizes a non-zero intermediate frequency (IF) type receiver, then the frequency of the IF must be known *a priori*.

A non-zero IF type receiver is proposed for the leakage signal detector in Fig. 2, where a non-zero IF can remove the ambiguity between the incoming leakage signal and detector's own leakage signal. The signal in the IF band is downconverted to baseband via quadrature mixing, as shown in Fig. 2.

III. Model of Detection Process

A mathematical model for the proposed detector is shown in Fig. 3. The downconverted leakage signal is an unmodulated tone, and the downconverted noise signal is modeled as a wide-sense stationary (WSS) bandpass random process. First, the downconverted leakage signal can be described by

$$l_B(t) = A_L \cos(\omega_B t + \theta_1) + jA_L \sin(\omega_B t + \theta_1) \qquad (1)$$

where A_L, ω_B, and θ_1 are the leakage signal amplitude, the downconverted leakage signal frequency, and an arbitrary phase, respectively. The phase information can be ignored in (1), because the proposed technique focuses on the magnitude response of the discrete fourier transformation (DFT), and so after sampling, (1) can be written as

$$l_B[m] = A_L \exp\left(\frac{j2\pi rm}{M}\right), \quad m \in [0,\ M-1] \qquad (2)$$

where M is the total number of samples of the DFT, and r denotes the frequency bin number for the downconverted leakage signal in the DFT, assuming for simplicity that ω_B is an integer multiple of the resolution frequency in the DFT.

The output of the DFT is given by

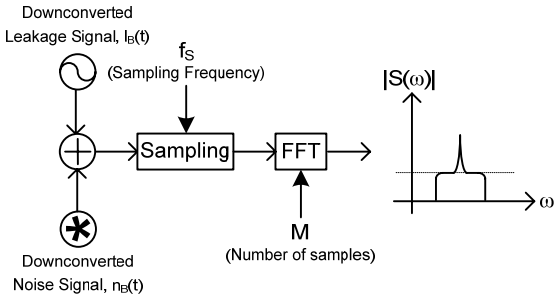

Fig. 3. Receiver model.

$$L[k] = \sum_{m=0}^{M-1} l_B[m] \exp\left(-j\frac{2\pi}{M}km\right). \qquad (3)$$

Using (2) in (3), we obtain

$$\begin{aligned} L[k] &= A_L e^{j\pi(r-k)\left(1-\frac{1}{M}\right)} \frac{\sin(\pi(r-k))}{\sin(\pi(r-k)/M)} \\ &= A_L M \delta[r-k] \end{aligned} \qquad (4)$$

where $\delta[\cdot]$ is the Kronecker delta function.

If the input to the system consists of thermal noise only, the downconverted noise signal in the IF band can be represented as

$$n_{IF}(t) = n_C(t)\cos(\omega_{IF} t + \theta_2) - n_S(t)\sin(\omega_{IF} t + \theta_2) \qquad (5)$$

where $n_C(t)$ and $n_S(t)$ are the inphase and quadrature components of $n_{IF}(t)$, and ω_{IF} and θ_2 denote the IF frequency and random phase, respectively [7]. From (5), the complex envelope of the noise is given by

$$n_B(t) = n_1(t) + jn_2(t) \qquad (6)$$

where $n_1(t)$ and $n_2(t)$ are given by

$$n_1(t) = n_C(t)\cos(\theta_2) - n_S(t)\sin(\theta_2) \qquad (7)$$

and

$$n_2(t) = -n_C(t)\sin(\theta_2) - n_S(t)\cos(\theta_2). \quad (8)$$

Since $n_{IF}(t)$ in (5) is a bandlimited white Gaussian process, so are $n_1(t)$ and $n_2(t)$, and they are independent because their cross-correlation is zero if θ_2 is uniformly distributed between 0 to 2π and the spectrum of $n_{IF}(t)$ is symmetric about $\omega = \omega_{IF}$. After sampling, the correlations between the M samples of $n_1[m]$ and $n_2[m]$ are described by the auto-correlation function of $n_1[m]$ and $n_2[m]$, given by

$$R[\tau] = \sigma_{IF}^2 \left(\frac{\sin(W\tau)}{W\tau} \right) \quad (9)$$

where W and σ_{IF}^2 denote the bandwidth in radians/second of the bandlimited white spectrum and the variance of $n_{IF}(t)$, respectively, and $\tau = \alpha T_S$, where $\alpha \in [0, M-1]$ and T_S denotes the sampling time.

The output of the DFT is given by

$$N[k] = \sum_{m=0}^{M-1} n_B[m] \exp\left(-j \frac{2\pi}{M} km \right). \quad (10)$$

The real and imaginary parts of $N[k]$ are summations of weighted random variables. Assuming Nyquist rate sampling, (9) is zero for all τ except $\tau = 0$, i.e., all M samples of $n_1[m]$ and $n_2[m]$ are independent, the real and imaginary parts of $N[k]$ are each independent Gaussian random variables with a mean of zero and variance of $\sigma_{IF}^2 M$, and the magnitude of $N[k]$ follows the Rayleigh distribution, given by

$$f_{|N[k]|}(x) = \frac{x}{\sigma_N^2} e^{-\frac{x^2}{2\sigma_N^2}} \quad (11)$$

where σ_N^2 is given by $\sigma_{IF}^2 M$ [8].

Now suppose that the input signal, $s(t)$, includes both the deterministic signal and random noise. Then, from (4) and (10), we have

$$S[k] = A_L M \delta[r-k] + \sum_{m=0}^{M-1} n_B[m] \exp\left(-j \frac{2\pi}{M} km \right). \quad (12)$$

All the frequency bins except r contain noise, so their magnitude responses are described statistically by (11). However, when k equals r, the leakage signal response of $A_L M$ is also present, so the magnitude response is described by the Rician pdf,

$$f_{|S[r]|}(x) = \frac{x}{\sigma_N^2} e^{-\frac{x^2 + (A_L M)^2}{2\sigma_N^2}} I_0\left(\frac{A_L M}{\sigma_N^2} x \right) \quad (13)$$

where $I_0(\cdot)$ denotes the zeroth order modified Bessel function [8].

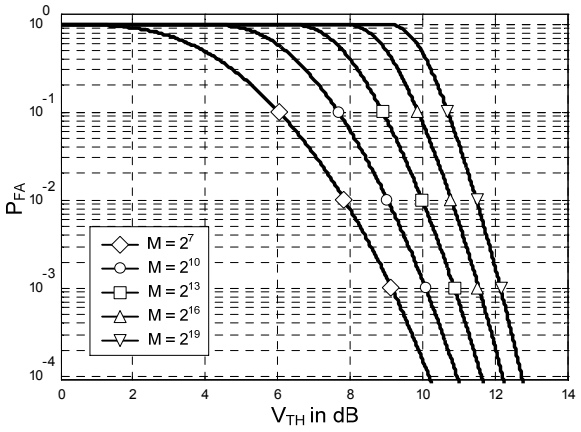

Fig. 4. Probability of false alarm (P_{FA}) as a function of threshold level (V_{TH}), parameterized by the number of samples (M).

IV. Detector Performance

The detector performance will be quantified in terms of the probability of false alarm (P_{FA}) and the probability of missed detection (P_{MD}).

A. Probability of False Alarm

A false alarm - or false detection of an MT - occurs when only noise is present at the input, but at least one of the DFT outputs exceed a predetermined threshold. This false alarm probability can be derived from (11).

We define a threshold as a predetermined value above the average level of all the frequency bins. Then, the probability that the noise does not exceed the threshold in a given frequency bin, denoted by P, equals

$$P = \int_{-\infty}^{V_{TH}+\mu_N} f_{|N[k]|}(x)\,dx = 1 - e^{-\frac{(V_{TH}+\mu_N)^2}{2\sigma_N^2}} \quad (14)$$

where V_{TH} and μ_N denote the predetermined decision threshold value and the average magnitude value of M noise bins, respectively. Then, P_{FA} is given by

$$P_{FA} = 1 - (P)^M = 1 - \left(1 - e^{-\frac{(V_{TH}+\mu_N)^2}{2\sigma_N^2}} \right)^M. \quad (15)$$

Fig. 4 plots P_{FA} versus V_{TH}, where the curves are parameterized by M.

B. Probability of Missed Detection

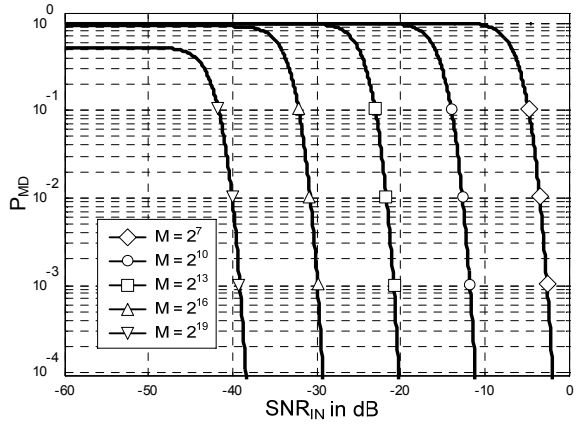

(a)

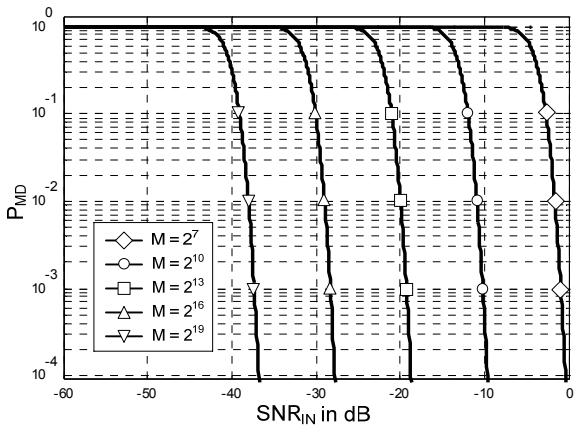

(b)

Fig. 5. Probability of missed detection (P_{MD}) as a function of input signal-to-noise ratio (SNR_{IN}), parameterized by the number of samples (M), with the threshold level (V_{TH}) of (a) 10 dB, (b) 13 dB.

A missed detection occurs when there is a leakage signal in at least one of the bins, but all of the magnitudes are below the threshold. Since each frequency bin can be described by one of the above two cases, i.e., one where only noise is present and the other where both signal and noise are present, the probability of missed detection is given by

$$P_{MD} = P_{E(\text{Signal pulse Noise bin})} \times \left(P_{E(\text{Noise bin})}\right)^{M-1} \tag{16}$$

where

$$P_{E(\text{Signal pluse Noise bin})} \triangleq \int_{-\infty}^{V_{TH}+\mu_S} f_{|S[r]|}(x)\,dx \tag{17}$$

$$P_{E(\text{Noise bin})} \triangleq \int_{-\infty}^{V_{TH}+\mu_S} f_{|N[k]|}(x)dx \tag{18}$$

and μ_S denotes the average magnitude of the $M-1$ noise bins and the signal-plus-noise bin. As a result, (16) can be rewritten as

$$P_{MD} = \left(1 - Q_M\left(\frac{A_L M}{2\sigma_N}, \frac{V_{TH}+\mu_N}{\sigma_N}\right)\right) \times \left(1 - e^{-\frac{\left(V_{TH}+\mu_N\right)^2}{2\sigma_N^2}}\right)^{M-1} \tag{19}$$

where $Q_M(\cdot)$ denotes the Marcum Q-function.

Since P_{MD} depends on the relative value of the signal and noise, the input signal-to-noise ratio (SNR_{IN}) defined by

$$SNR_{IN} = \frac{A_L^2}{2\sigma_{IF}^2} \tag{20}$$

is useful in evaluating (19). P_{MD} given by (19) is shown as a function of SNR_{IN} with two sample V_{TH} levels, 10 and 13 dB, in Fig. 5, where the curves are parameterized by M, and a noise bandwidth of 200 kHz and a detector Noise Figure of 3 dB are assumed.

C. Detector Sensitivity

The overall detector performance is determined by P_{FA} and P_{MD}. In order to control the detector sensitivity, the proposed detection technique has two critical variables, the number of samples (M) and the decision threshold level (V_{TH}). From Figs. 4 and 5, it is seen that P_{FA} is inversely proportional to V_{TH}, but proportional to M. However, P_{MD} is proportional to V_{TH}, but inversely proportional to M. Therefore, there is a tradeoff between P_{FA} and P_{MD} when adjusting M and V_{TH}.

The receiver operating characteristic (ROC) is useful in illustrating the detector sensitivity, since the ROC displays curves of ($1-P_{MD}$), the probability of correct detection, versus P_{FA}. Fig. 6 plots the ROC curves with values of M of 2^{13} and 2^{14}. In order to detect the small leakage power of –70 to –90 dBm, from 2^{14} to 2^{21} samples will be required for both P_{FA} and P_{MD} equal to 10^{-3} under the conditions of a path loss of 70 dB and a detector Noise Figure of 3 dB, as shown in Fig. 7.

V. CONCLUSION

A detection technique has been proposed to identify the presence of nearby WiMAX MT devices within the UWB communication range. The proposed technique is useful

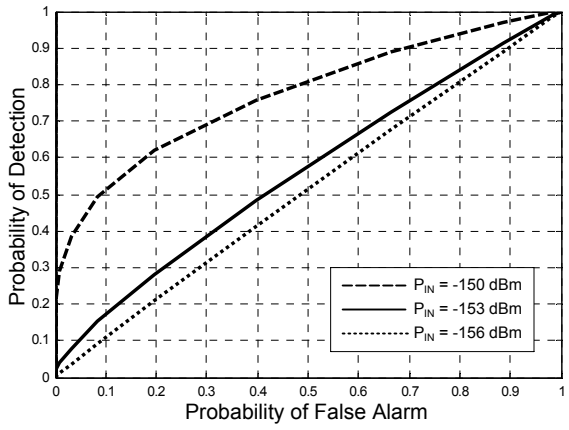

(a)

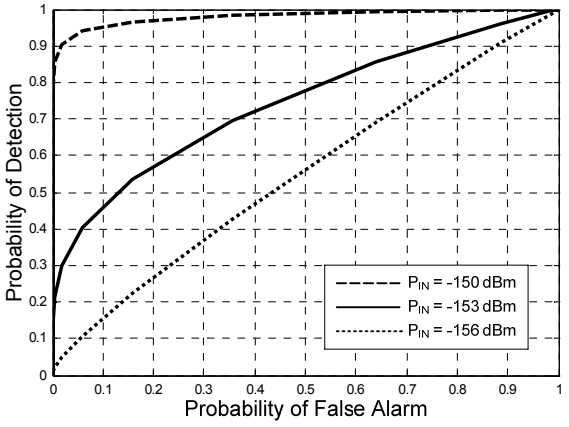

(b)

Fig. 6. Receiver operating curves (ROC) with a noise bandwidth of 200 kHz, a detector Noise Figure of 3 dB, and the number of samples of (a) 2^{13}, (b) 2^{14}.

when a UWB device scans the occupied WiMAX bands within the UWB communication range before transmitting. It was shown that the detector sensitivity can be adjusted by varying the number of samples and the decision threshold level. Practical issues, such as the required number of samples, the effects of phase noise, and the determination of realistic leakage power levels, require further study.

ACKNOWLEDGMENT

The authors would like to acknowledge the support of the UCSD Center for Wireless Communications, as well as the UC Discovery Grant Program. The authors would also like to thank Dr. J. Foerster at Intel for many useful technical discussions.

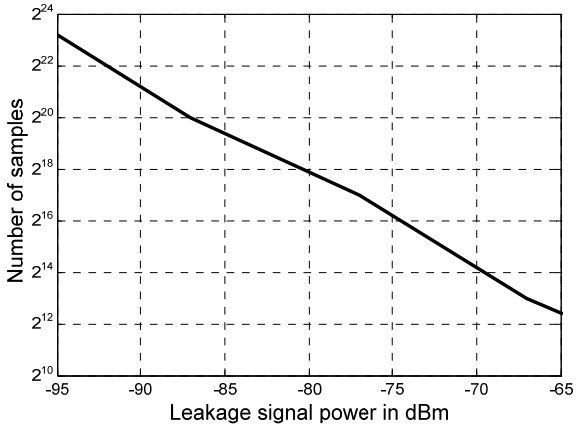

Fig. 7. Number of samples required for P_{FA} and $P_{MD} = 10^{-3}$ as a function of leakage signal power, under the conditions of a path loss of 70 dB and a detector Noise Figure of 3 dB.

REFERENCES

[1] FCC, "First report and order, revision of part 15 of the commission's rules regarding ultra-wideband transmission systems," ET Docket pp. 98-153, Feb. 14, 2002.

[2] WiMAX Forum, "Regulatory position and goals of the WiMAX FORUM," Aug. 2004, available online: http://www.wimaxforum.org/news/downloads/WiMAX_Forum_Regulatory_Whitepaper_v08092004.pdf.

[3] *Specification of the IEEE Std 802.16™*, 2004.

[4] R. S. Wolff, "An assessment of the potential terrestrial interference due to direct broadcast satellite television receivers," *IEEE J. Select. Areas Commun.*, vol. SAC-3, no. 1, pp. 148-154, Jan. 1985.

[5] G. J. M. Janssen, P. A. Stigter, R. Prasad, "Wideband indoor channel measurements and BER analysis of frequency selective multipath channels at 2.4, 4.75, 11.5 GHz," *IEEE Trans. Commun.*, vol. 44, no. 10, Oct. 1996.

[6] http://www.bushywood.com/tv_detector_vans.htm.

[7] R. E. Ziemer, W. H. Tranter, *Principles of Communications, Systems, Modulation, and Noise*, 5th ed., New York: John Wiley & Sons, 2002.

[8] P. Z. Peebles, Jr., *Probability, Random Variables, and Random Signal Principles*, 3rd ed., New York: McGraw-Hill, 1993.